JOURNAL OF MATERIALS SCIENCE 17 (1982) 1825–1833

The observation of stress effects during the high temperature oxidation of iron

T. E. MITCHELL, D. A. VOSS*, E. P. BUTLER†
Department of Metallurgy and Materials Science, Case Western Reserve University, Cleveland, Ohio 44106, USA

Electron microscopy has been used to characterize the stress effects which occur during the oxidation of iron in the temperature range 400–700° C. Spalling and de-cohesion of the outer hematite (α-Fe_2O_3) layer is often observed, and analysis of the resulting scrolled oxide indicates a strong compressive stress gradient. In contrast, tensile cracks are frequently seen in the magnetite (Fe_3O_4) layer, while the underlying wustite ($Fe_{1-x}O$) and the iron substrate are apparently able to accommodate the stresses to some extent by plastic deformation. The Pilling–Bedworth model can adequately be applied at the α-Fe_2O_3–Fe_3O_4 interface since anion diffusion occurs in the hematite. However, since cation diffusion is dominant in the other oxides, it is suggested that the anion volume ratio can be applied to the Fe_3O_4–$Fe_{1-x}O$ interface where the anion sublattice remains unchanged, in order to predict the stress state.

1. Introduction

The origin and consequences of stress effects which occur during the oxidation of metals are subjects in which there is considerable interest and controversy [1, 2]. For a metal oxidizing by anion diffusion, stresses result as new oxide is produced at the oxide–metal interface. Under these conditions the volumetric change between metal and oxide, expressed via the Pilling–Bedworth Ratio (PBR) [3], can be used to predict the localized stress state. For a metal oxidizing by the usual case of cation diffusion, however, no such simple considerations are possible; new oxide is formed at the oxide–oxygen free-surface, and both oxide and metal should therefore be stress-free. That this is not so has been clearly demonstrated throughout the literature, but no satisfactory explanation has been advanced, even for metals with a single oxide layer. In the case of iron, the formation of three oxide layers during high temperature ($> 570°$ C) oxidation causes a complex stress state which often results in cracking and spalling of the oxides, leading to further enhanced oxidation [4]. The principal oxide formed, wustite, $Fe_{1-x}O$, has outer layers of Fe_3O_4 and α-Fe_2O_3 which, although comprising less than 10% of the total oxide scale, nevertheless exert a strong influence on the bulk scaling behaviour during oxidation. However, it is the stress state at the inner wustite–iron interface which is of primary interest because adherence or loss of adherence at this location greatly affects the oxidation kinetics and generally determines the oxidation resistance of the metal. Loss of adherence has been shown by thermo-gravimetric measurements [5] to slow down the rate of oxidation significantly if spalling and re-oxidation can be prevented. Important processes which must be considered in discussions of stress effects and the adherence of scales produced through cation oxidation include stress generation, vacancy condensation and vacancy injection.

One possible explanation for the de-cohesion of an oxide is that extensive stresses are generated at the oxide–metal interface during growth and so the oxide breaks away in order to relieve these stresses. Evidence for the existence of these growth stresses come from the observation of deformation during the oxidation of Fe coils [6] and the effect

*Present address: Powell Metals and Chemicals Inc., P.O. Box 5646, Rockford, Ill. 61125, USA.
†Permanent address: Department of Metallurgy and Materials Science, Imperial College, London, SW72BP, England, UK.

0022–2461/82/061825–09$03.58/0 © *1982 Chapman and Hall Ltd.*

of Fe_3O_4 and α-Fe_2O_3 formation on the oxide scale plasticity [7]. In addition Noden *et al.* [8] showed that considerable creep, due to tensile stresses in the metal, occurred in stainless steel fuel pins when exposed to air at 900° C, and Dankov and Churaev [9] characterized a compressive stress in $Fe_{1-x}O$ during oxidation, thus also implying a tensile stress in the Fe. An alternative explanation for loss of adherency is possible, based on vacancy condensation. These defects, created via the outward cation diffusion process, can condense at the oxide–metal interface after the substrate has become saturated, forming small voids. The growth and agglomeration of these voids can then lead to local de-cohesion of the oxide [5].

The arguments for mechanisms based on vacancy injection have yet to be substantiated microstructurally. However, several experiments on bulk Fe samples have provided indirect evidence in support of this idea. Dunnington *et al.* [10], for example, noticed that during oxidation of thin Fe sheets one side of the sheet formed an adherent scale but the opposite side invariably formed a loose, non-adherent layer. This observation was interpreted to mean that vacancies are injected at the adherent oxide–iron interface and subsequently diffuse through the Fe to the opposite side of the thin sample where they are absorbed. During the early stages of oxidation, vacancies are injected into the metal from both sides of the sheet; the sheet soon becomes saturated with vacancies and lose adherence. After this point, the adherent oxide grows at the expense of the non-adherent oxide, freely injecting vacancies into the Fe substrate. Similar experiments on Fe sheets were reported by Tylecote and Mitchell [11], substantiating this work. In addition, these investigators created artificial vacancy sinks in the Fe by drilling small holes in the Fe sheet near the gas–metal interface, before oxidation. The experiment was designed to prevent oxidation in and around the holes, and upon oxidation, a strongly adherent oxide scale was formed on both sides of the specimen. The holes in the specimen became enlarged and assumed a distinctly oval shape, the long side of the oval being normal to the oxide–metal interface. If growth of the holes had been a result of stresses in the Fe, the long axis of the oval would be parallel to the oxide–iron interface. The iron oxide scale is known to remain adherent for longer times on bulk than on thin Fe samples [10]. Both of the previous authors interpret this to mean that thicker Fe specimens can absorb more vacancies before becoming saturated, and, therefore, before commencing exfoliation. This interpretation is capable of being extended to explain the increase in oxidation rate due to cold-working [12]. The increase in dislocation density not only provides more sinks for injected vacancies, but also provides for more rapid diffusion and better distribution of the vacancies, thus delaying saturation in the Fe substrate. The longer adhesion of the oxide scale results in faster oxidation kinetics.

Harris [13] has challenged the importance of the vacancy injection process during cation oxidation, considering that vacancies are generally destroyed at the metal–oxide interface. Void formation in metals during oxidation was re-interpreted via the Hull–Rimmer creep mechanism. Cagnet and Moreau [14] claim to have observed fine pores in the Fe below the oxide–iron interface after oxidation, but to the present authors' knowledge this is the only published evidence of void formation in Fe during oxidation. If one considers the numerous optical microscope studies on the oxidation of Fe which have failed to show any void formation in Fe, one must conclude that the arguments of Harris do not pertain to the Fe–O system.

In the present investigation oxidized iron surfaces have been examined by scanning electron microscopy (SEM) at stages where their adherency to the substrate is beginning to break down. Analysis of these configurations provides insight as to the stress distribution in the oxides near the surface of the iron oxide scale. In addition the oxide-iron interface has been studied using trans-

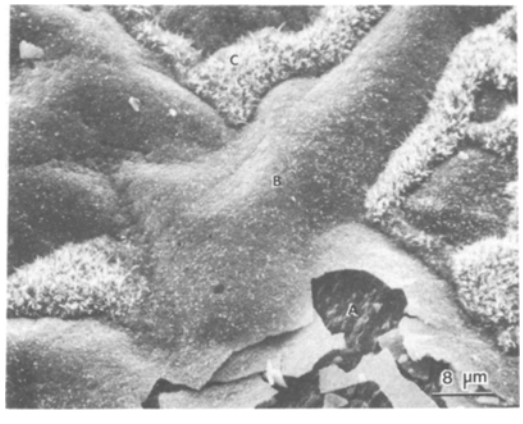

Figure 1 Scanning electron micrograph showing α-Fe_2O_3 de-cohesion and cracking, A, blistering, B, and blade growth, C, during the early period of oxidation (sample oxidized for 5 min at 600° C).

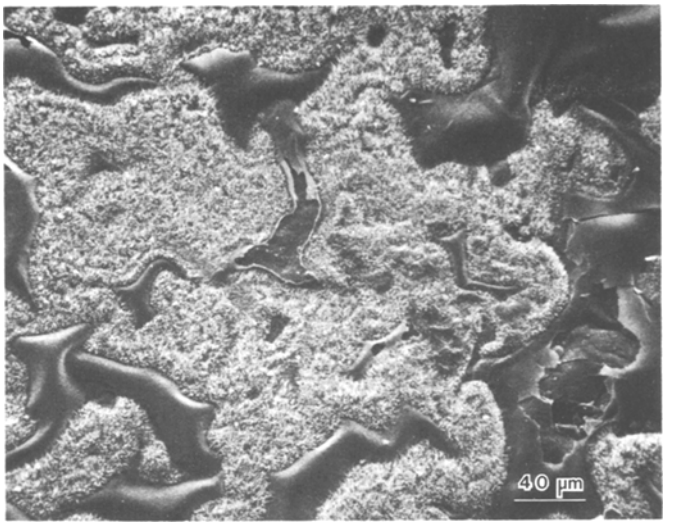

Figure 2 Scanning electron micrograph showing areas of dense α-Fe_2O_3 blade growth surrounding blistered areas which exhibit no blade formation. Blistering must have occurred during oxidation for 2 h at 600° C.

mission electron microscopy techniques to provide a more complete characterization of the stress state in the iron oxide scale. Other papers in this series have described the hematite blades which grow from the oxidized surface of iron [15] and the epitaxial relationships and overall microstructures which are observed during the high temperature oxidation of iron [16].

2. Experimental techniques

Fully annealed 99.998% pure iron was oxidized in 20 torr of flowing O_2 at temperatures from 400 to 700° C following procedures described elsewhere [17]. Oxide surfaces were studied by SEM after routine mounting and carbon coating of the sample.

The back-polishing technique [18] was used to prepare specimens for TEM study near the oxide–iron interface. 3 mm discs (~ 0.25 mm thick) were oxidized for short times in order to develop a thin oxide coating. The discs were then electropolished from one side in a solution of glacial acetic acid and 70% perchloric acid in 20:1 ratio. The back-polished sample was ion-thinned in order to assure electron transparency near the oxide–iron interface.

3. Results

Examination of oxidized iron specimens revealed that spalling and de-cohesion were most apparent in the 600° C oxidation, possibly as a result of the newly formed $Fe_{1-x}O$ phase. All specimens showed areas where de-cohesion and blistering of the surface oxide had occurred, as well as areas of continued adherence where blades of α-Fe_2O_3 formed.* Fig. 1, from a 5 min oxidation, indicates that both de-cohesion and blade formation occur during the early minutes of oxidation. Fig. 2 shows similar blistering after a longer oxidation (2 h), so that a much thicker carpet of α-Fe_2O_3 has grown on the adherent areas surrounding the blisters. It is possible to interpret blistering and spalling of an oxide layer on samples cooled from the oxidation temperature as being due to differ-

Figure 3 Scanning electron micrograph of the blade–blister interface. Note porosity in the blistered oxide formed at $T = 600°$ C after 2 h oxidation.

*Hematite blades grow out of the oxide surface by the surface diffusion of cations up tunnels along the axes of the blades [15].

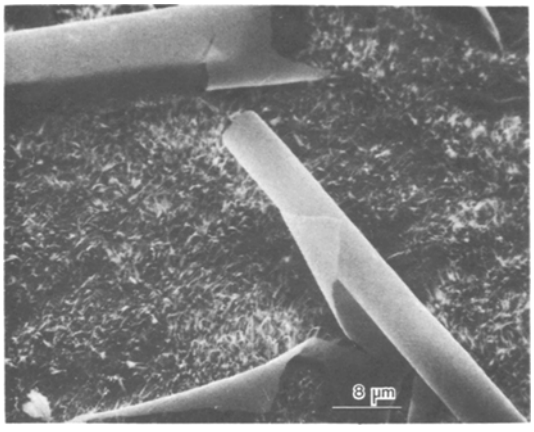

Figure 4 Scanning electron micrograph of the thin surface oxide (α-Fe_2O_3) which has curled into a scroll as the compressive growth stresses were relieved by de-cohesion. Oxidized at 600° C for 30 min.

ences in the thermal expansion coefficients between oxide and metal. Tien and Davidson [19] have reviewed oxide spallation mechanisms arising from such temperature changes and heat transfer considerations. However, in iron, the α-Fe_2O_3 blades grow in areas surrounding the blisters, so it is evident that de-cohesion must have occurred during the oxidation period as a result of growth stresses. If the scale had remained adherent until the quench, the hematite blades would have formed on the blister surfaces as well, but this is not the case, as shown in Fig. 3, which is a direct overhead view of the abrupt hematite blade–porous oxide (blister) interface. Optical microscopy indicated that the blistering observed at the surface results from loss of adherency of the α-Fe_2O_3 layer from the Fe_3O_4 substrate. These blisters, therefore, are caused by large compressive stresses in the α-Fe_2O_3 layer which arise during growth of the α-Fe_2O_3 out of the Fe_3O_4.

In Fig. 4, the α-Fe_2O_3 layer is seen to have delaminated at one edge and curled up into a scroll as a result of the compressive stress gradient through the α-Fe_2O_3 layer. The curled oxide is extremely thin (~ 25 nm) and de-cohesion must have occurred early in the oxidation because the blades are equally dense in the area exposed by the curl as in the regions of adherence. This micrograph illustrates the consequences of an elastic stress–strain gradient existing across a single oxide phase when it remains adherent to its substrate; the largest stress is at the oxide–substrate interface and the minimum stress is zero at the surface. The direction of the curl after de-cohesion indicates that the maximum compressive stress is present at the oxide–substrate interface before de-cohesion. One can estimate roughly the magnitude of this stress by assuming that the curl is pure bending and that there is a totally elastic stress distribution as shown in Fig. 5. At the adherent α-Fe_2O_3–Fe_3O_4 interface, the difference in strain with respect to the oxide–gas interface, $\Delta\epsilon_y$, is

$$\Delta\epsilon_y = (o-y)/\rho = \frac{-25.0\,\text{nm}}{3.5\,\mu\text{m}} = 0.007 \quad (1)$$

where y is the thickness and ρ is the radius of curvature (Fig. 5). Since the elastic modulus, E, of $Fe_2O_3 = 2.15 \times 10^{11}$ N m^{-2} [20], the maximum compressive modulus, σ_{max}, is

$$\sigma_{max} = E\Delta\epsilon_y \sim 1500\,\text{MN m}^{-2}. \quad (2)$$

This simple calculation shows that the maximum adherency strain at the interface is 0.7% and that the stress gradient across the hematite is enormous. Presumably the compressive stress is

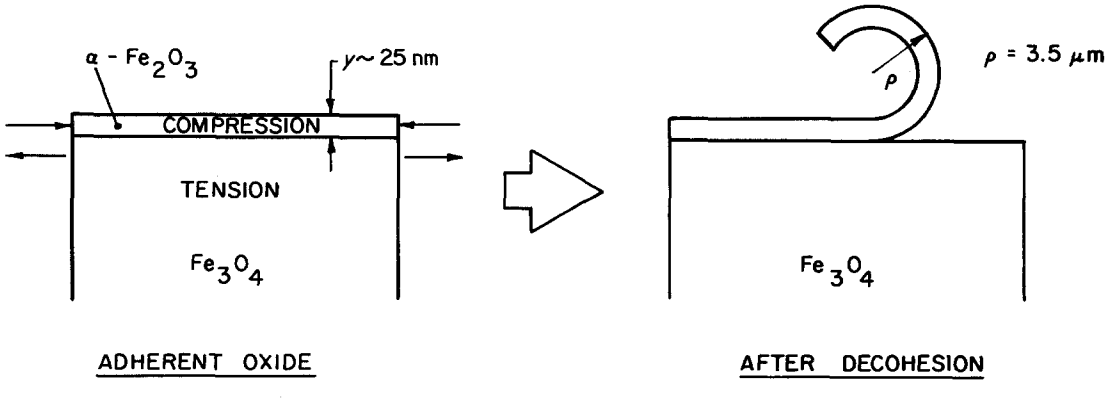

Figure 5 Schematic diagram of the stress states and dimensional parameters associated with the formation of α-Fe_2O_3 scrolls.

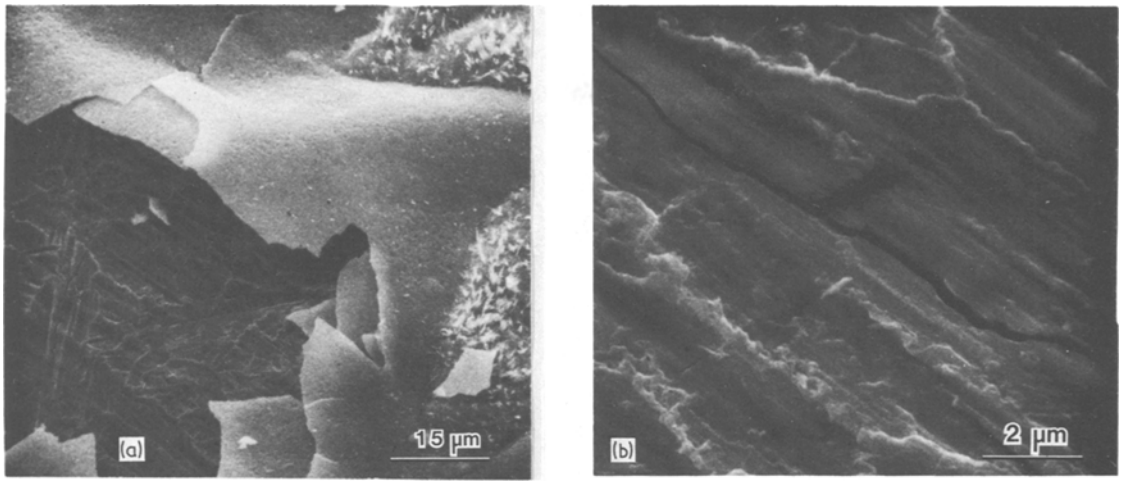

Figure 6 Scanning electron micrographs of a blistered and spalled oxide area following oxidation at 600° C for 10 min showing (a) general area, (b) a crack in the underlying Fe_3O_4 layer arising from tensile stresses.

relieved first of all by blistering so that the resulting tensile stress in the outer layer leads to cracking and then scrolling. The high stress is apparently insufficient to deform the hematite plastically. This is consistent with the behaviour of alumina (α-Al_2O_3) which is isomorphous with hematite and has a brittle-to-ductile transition at approximately 1000° C [24].

The scanning electron micrographs in Fig. 6 complete this graphical description of the stress distribution at the Fe_2O_3–Fe_3O_4 interface. In Fig. 6a, the blistered α-Fe_2O_3 layer has failed under compression in a buckling mode. The spalling and cracking of the scale permits observation of the underlying oxide, Fe_3O_4. In Fig. 6b, a tensile crack is apparent in the Fe_3O_4 layer. Consideration of the stress equilibrium at the α-Fe_2O_3–Fe_3O_4 interface suggests that an opposing tensile stress should exist in the Fe_3O_4 layer when a compressive stress is observed in the α-Fe_2O_3. The striations which appear in the area around the crack underneath the spall, are probably caused by the plastic deformation associated with the α-Fe_2O_3 layer pulling away from the Fe_3O_4. Much smaller cracks were observed in the Fe_3O_4 using TEM, Fig. 7. In samples oxidized for only a short time and then back-polished, there was evidence for plastic deformation in the iron substrate adjacent to the oxide interface (Fig. 8). Note that, in Fig. 8, the oxide that forms first is Fe_3O_4, even though the oxidation temperature (600° C) is within the wustite stability regime. As explained elsewhere [16], this is because the oxygen pressure is high enough for magnetite to be more stable; at longer oxidation times wustite would form at the Fe_3O_4–Fe interface.

4. Discussion

The experimental evidence presented in this paper requires examination in light of several important factors. Firstly, Mackenzie and Birchenall [7] showed that $Fe_{1-x}O$ will creep under stresses that

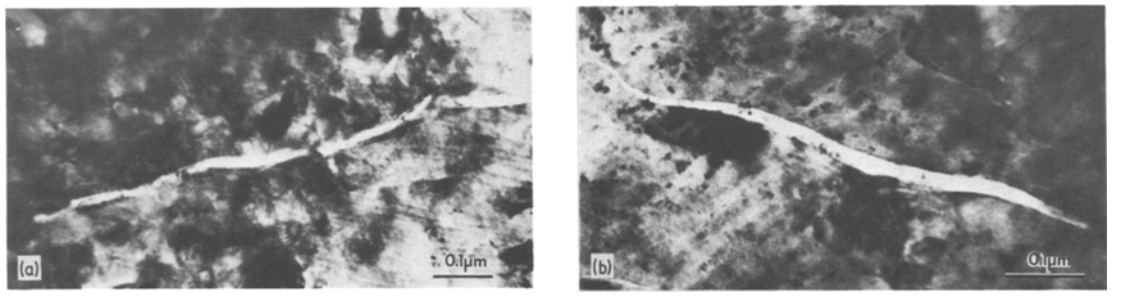

Figure 7 Bright field electron micrographs showing cracks resulting from the tensile stresses in the Fe_3O_4 layer after oxidation at 500° C for 1 h (a) in a fine grain polycrystalline region, and (b) in a single crystal region.

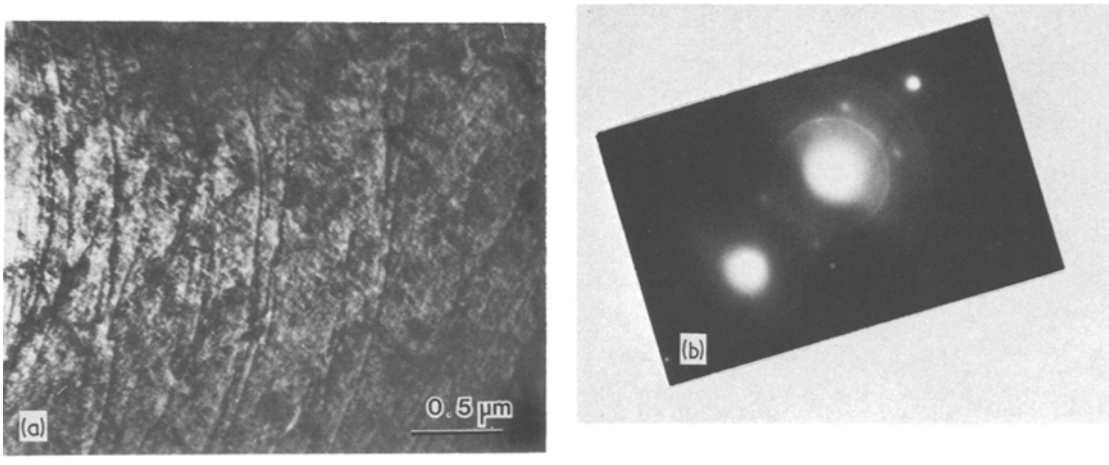

Figure 8 (a) Bright field electron micrograph showing dislocations in the iron substrate that were generated via stresses at the Fe_3O_4–Fe interface during early (5 min) oxidation at 600° C, (b) selected area diffraction pattern of (a) showing rings corresponding to polycrystalline Fe_3O_4 and operating g vector (211).

do not deform the higher oxides. The ability of the thick $Fe_{1-x}O$ layer to creep and deform at the oxidation temperature, and thus to relieve stresses, implies that the growth stress in this layer will be small. Consideration of the rapid Fe diffusion rate in $Fe_{1-x}O$ leads to this same conclusion. Secondly, many researchers have observed that the entire iron oxide scale spalls during rapid cooling of the specimen due to differences in thermal expansion coefficients between iron and the oxides. However, all of the stress related observations described here, with the possible exception of the interface dislocations generated in the Fe, must have occurred during oxidation and prior to rapid cooling of the specimen.

The origin of stresses in growing oxide films has been considered by a number of investigators. Jaenicke and Leistikow [22] suggested that recrystallization in the oxide scale results in development of stresses, but the recrystallization process itself is usually thought to be a stress relief mechanism. Similarly, Rhines and Wolfe [23] have developed a growth stress theory based on observations with nickel, whereby internal growth occurs within an already continuous oxide layer. It was assumed that oxygen diffuses along the oxide grain boundaries or cracks in the oxide and reacted with Ni^{2+} ions diffusing in the bulk oxide. They reasoned that this causes excessive amounts of oxide to form at the boundaries and creates a compressive stress in the oxide scale. Speight and Harris [21] have clearly demonstrated that this mechanism is untenable; such boundary oxide can relax existing applied external stresses but cannot create stresses nor augment existing ones. One might argue therefore that the only stress generation mechanism during oxidation which is justifiable is that based upon an orientation relationship between an oxide and its substrate. If adherency is to be maintained at an interface between two phases, oxide–oxide or oxide–metal, elastic strain will exist in both phases at the interface. The observation of a scrolled oxide after de-cohesion suggests a maximum stress at the interface, i.e., a growth stress originating at an interface. Whereas plastic flow occurs to relieve the stresses in Fe and $Fe_{1-x}O$, the oxidation temperatures are almost certainly below the brittle-to-ductile transition temperatures of both Fe_3O_4 and Fe_2O_3.

Epitaxially induced stresses which originate at the phase interface led to the development of the growth stress theory by Pilling and Bedworth [3] based on the volume strain resulting from atomic volume differences between the two structures. The Pilling–Bedworth Ratio (PBR) compares the volume occupied by a metal atom in the oxide to the volume occupied by a metal atom in the substrate:

$$\text{PBR} = \frac{\text{volume per metal atom in oxide}}{\text{volume per metal atom in substrate}} \quad (3)$$

TABLE I Unit cell data at room temperature for iron and its oxides

Phase	Lattice	Lattice parameters (nm)	Formula units per unit cell, M	Volume per Fe atom, V_{Fe} ($\times 10^{-3}$ nm^3)	Volume per O atom, V_O ($\times 10^{-3}$ nm^3)
Fe	Cubic	$a = 0.286\,64$	2	11.78	–
$Fe_{0.94}O$*	Cubic	$a = 0.4308$	4	21.26	19.99
$Fe_{0.90}O$†	Cubic	$a = 0.4291$	4	21.94	19.75
Fe_3O_4	Cubic	$a = 0.839\,40$	8	24.64	18.48
α-Fe_2O_3	Hexagonal	$a = 0.503\,45$ $c = 1.3749$	6	25.15	16.77

*Composition of wustite in equilibrium with Fe at ~ 800° C [26].
†Composition of wustite in equilibrium with Fe_3O_4 at ~ 800° C [26].

This ratio predicts firstly the sign, and secondly estimates the relative magnitude, of the stress in the oxide to be proportional to (1-PBR). A ratio of less than 1 is indicative of a cellular porous oxide in tension whereas a ratio greater than 1 indicates a compact or compressed oxide which should result in a slow oxidation rate based on bulk diffusion in the oxide. One should note that this expression assumes that oxygen is the only mobile species in the oxide, a relatively uncommon condition in metal oxidation. Although the reasons are poorly understood, this expression nevertheless shows good qualitative agreement with experimentally observed stresses in oxide scales.

The various crystal data used for calculating volume changes are shown in Table I for iron and its oxides and the volume ratios are summarized in Table II. For example, since the Pilling–Bedworth approach should apply only when oxygen is the diffusing species, it can reasonably be used at the α-Fe_2O_3–Fe_3O_4 interface where this situation holds. Here we can use the data in Table I:

$$\text{PBR} = \frac{V_{Fe}(\alpha\text{-}Fe_2O_3)}{V_{Fe}(Fe_3O_4)} = \frac{25.15}{24.64} = 1.02 \quad (4)$$

where V_{Fe} is the volume of oxide per Fe atom; this predicts that there will be a compressive stress in the α-Fe_2O_3 layer and a tensile stress in the Fe_3O_4, in agreement with the observed growth stresses (see Table II). The predicted 2% volume strain corresponds to a 0.7% linear strain which is in fortuitously close agreement with the strain estimate from the curl of the hematite scrolls in Section 3. At the Fe_3O_4–$Fe_{1-x}O$ interface, where Fe is the rapidly diffusing species, it is difficult to understand how the difference in volume occupied by an Fe atom could have any physical significance in determining a stress at the interface. However, it makes sense to modify the Pilling–Bedworth criterion to take into account the unchanging oxygen positions and express this as the anion volume ratio (AVR). At this interface we estimate, using the data of Table I:

$$\text{AVR} = \frac{V_0(Fe_3O_4)}{V_0(Fe_{1-x}O)} = \frac{18.48}{19.75} = 0.94 \quad (5)$$

where V_0 is the volume of oxide per oxygen atom. This ratio, being less than 1, predicts that there will be a tensile stress in the Fe_3O_4 and a compressive stress in the massive $Fe_{1-x}O$ layer. Hence observations of a compressive failure mode in the thin hematite layer and the tensile crack (Fig. 6) which appears to extend entirely through the magnetite layer as a result of tensile stresses arising at both of the Fe_3O_4 interfaces are consistent with this modelling.

Stresses generated in the $Fe_{1-x}O$ and Fe substrate can be relieved; the Fe can deform plastically (as Fig. 8 indicates) and the $Fe_{1-x}O$ layer is known to creep extensively during high temperature oxidation [7]. Therefore, any stresses generated at the $Fe_{1-x}O$ interface should be short range and the

TABLE II A consideration of the Pilling–Bedworth model for stress in growing iron oxide films

Interface (Higher Oxide–Lower Oxide)	(1-PBR)* (Fe lattice O^{2-} diffusing)	(1-AVR)* (O lattice Fe^{2+} diffusing)	Observed growth stresses
$Fe_{1-x}O$/Fe	−0.80	–	
Fe_3O_4/Fe	−1.09	–	
Fe_3O_4/$Fe_{1-x}O$	−0.12	+0.006	Tension in Fe_3O_4
α-Fe_2O_3/Fe_3O_4	−0.02	+0.09	Compression in α-Fe_2O_3

*Negative values indicate compression in higher oxide, tension in substrate. Positive values indicate tension in the higher oxide, compression in substrate.

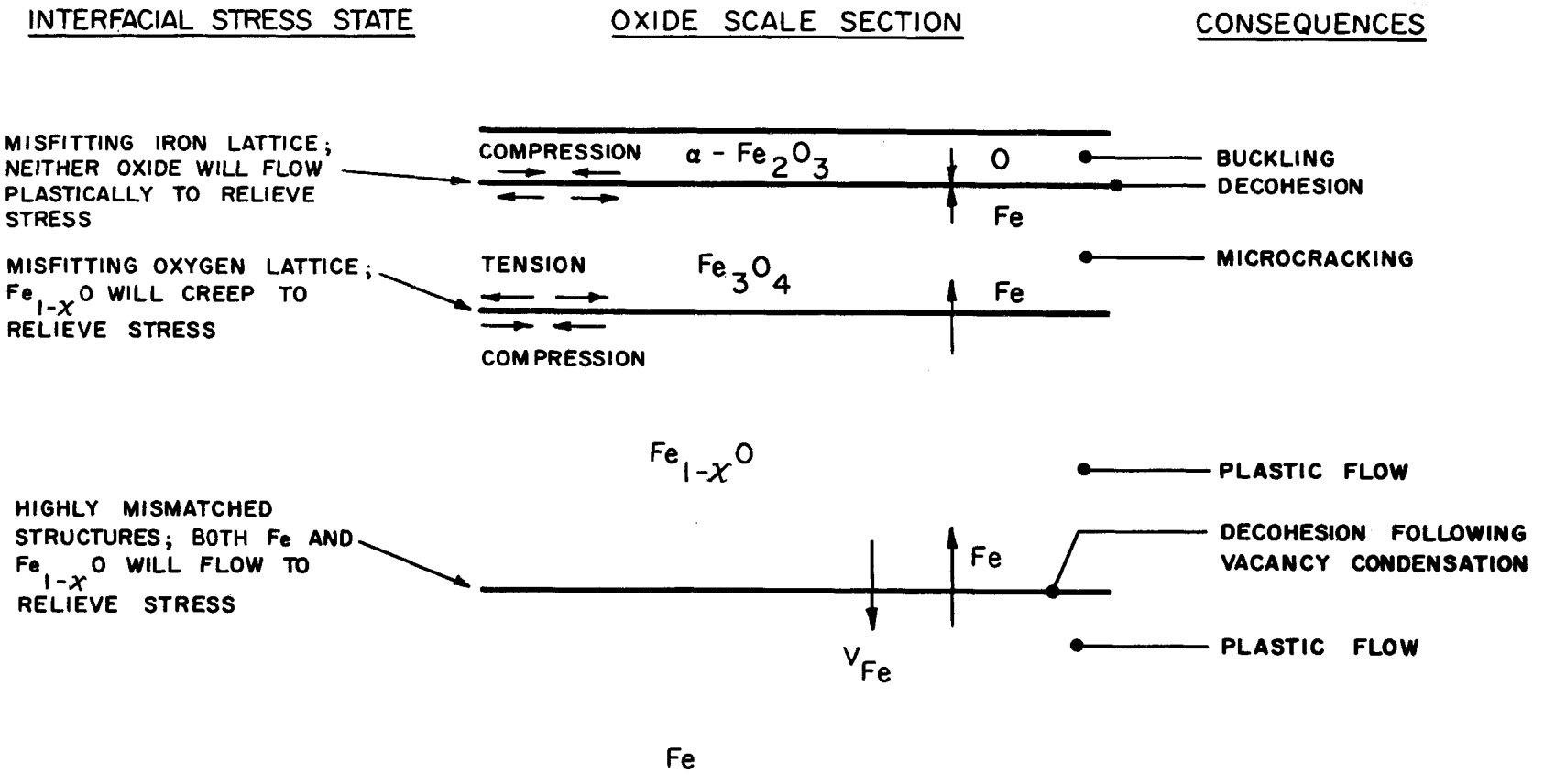

Figure 9 Sketch of iron oxide stress states and their consequences.

thick $Fe_{1-x}O$ layer should act as a buffer between the highly stressed surface oxides and the Fe. For these reasons it is difficult to explain de-cohesion at the $Fe_{1-x}O$ interface during oxidation as a result of any type of growth stress acting on that interface. Instead, it seems logical to conclude that loss of adherency of the oxide scale is caused by vacancy condensation, after the Fe matrix has become locally saturated with vacancies. The reported preferential loss of adherency near the corner of an oxidized sample [6, 7, 25] is consistent with this mechanism. Near a corner or short edge a proportionally larger surface area is available to the oxide to inject vacancies and it is likely that vacancy saturation will first occur in this localized metal volume, thus causing loss of adherency of the scale.

The diagram in Fig. 9 summarizes the proposed stress distribution in the iron oxide scale, and Table II summarizes the Pilling–Bedworth model in both its original and modified forms as it relates to the iron oxide scales.

5. Conclusion

Spalling and de-cohesion of the thin upper layers of iron oxide result in enhanced oxidation rates, although not as much as result from de-cohesion at the $Fe_{1-x}O$–Fe interface during high temperature oxidation. The micrographs presented here illustrate that stresses through the oxide scale arise at the oxide interfaces and they are extremely large, large enough to fracture magnetite in tension and to deform hematite significantly in compression. However, the stress–strain gradients in a single adherent oxide layer (α-Fe_2O_3) are elastic and, when relieved by de-cohesion, permit extensive deformation of the oxide layer. At the oxide–iron interface plastic deformation of the iron substrate occurs to accomodate the $Fe_{1-x}O$ growth stresses.

The blades of α-Fe_2O_3 which are often observed on oxidized Fe surfaces require an adherent surface oxide to provide a large source of Fe cations for their growth. Their presence or absence and relative density can be used to order chronologically the events occuring during oxidation. This reasoning suggests that de-cohesion of the surface oxide occurs during growth at the oxidation temperature and not during rapid cooling from the oxidation temperature.

Acknowledgements

This research was supported by the National Science Foundation through CWRU Materials Research Laboratory Grant No. DMR 78–24150.

References

1. J. STRINGER, *Corrosion Sci.* **10** (1970) 513.
2. J. V. CATHCART (ED.), "Stress Effects and the Oxidation of Metals" (AIME, New York, 1975).
3. N. B. PILLING and R. E. BEDWORTH, *J. Inst. Met.* **29** (1923) 529.
4. D. BRUCE and P. HANCOCK, *J. Iron Steel Inst.* **11** (1970) 1021.
5. D. CAPLAN, G. I. SPROULE and R. J. HUSSEY, *Corrosion Sci.* **10** (1979) 9.
6. H. ENGELL and F. WEVER, *Acta Met.* **5** (1957) 695.
7. J. D. MACKENZIE and C. E. BIRCHENALL, *Corrosion* **13** (1957) 783.
8. J. D. NODEN, C. J. KNIGHTS and M. W. THOMAS, *Brit. J. Corrosion* **3** (1968) 47.
9. D. D. DANKOV and P. V. CHURAEV, *Dolk. Akad. Nauk. SSSR* **73** (1950) 1221.
10. B. W. DUNNINGTON, F. H. BECK and M. G. FONTANA, *Corrosion* **8** (1952) 2.
11. R. F. TYLECOTE and T. E. MITCHELL, *J. Iron Steel Inst.* **196** (1960) 445.
12. D. L. CARPENTER and A. C. RAY, *Corrosion Sci.* **13** (1973) 493.
13. J. E. HARRIS, *Acta Met.* **26** (1978) 1033.
14. M. CAGNET and J. MOREAU, *Compt. Rend. Acad. Sci. Paris* **244** (1957) 2924.
15. D. A. VOSS, E. P. BUTLER and T. E. MITCHELL, *Met. Trans.* in press.
16. K. KURODA, E. P. BUTLER, D. A. VOSS and T. E. MITCHELL, to be published.
17. D. A. VOSS, M.S. Thesis, Case Western Reserve Univ., Cleveland, Ohio (1979).
18. G. M. SCAMANS and E. P. BUTLER, *Met. Trans.* **6A** (1975) 2055.
19. J. K. TIEN and J. M. DAVIDSON, in "Stress Effects and the Oxidation of Metals", edited by J. V. Cathcart (AIME, New York, 1975) p. 200.
20. J. B. WACHTMAN (ED)., "Mechanical and Thermal Properties of Ceramics" (NBS Special Publication 303, 1969) p. 146.
21. M. V. SPEIGHT and J. E. HARRIS, *Acta Met.* **26** (1978) 1043.
22. W. JAENICKE and S. LEISTIKOW, *Z. Phys. Chem.* **15** (1958) 175.
23. F. N. RHINES and J. S. WOLF, *Met. Trans.* **1** (1970) 1701.
24. T. E. MITCHELL, *J. Amer. Ceram. Soc.* **62** (1979) 254.
25. F. W. JUENKER, R. A. MEUSSNER and C. E. BIRCHENALL, *Corrosion* **14** (1958) 57.
26. E. BAUER, A. PIANDLI, A. AUBRY and F. JEANNOT, *Mater. Sci. Bull.* **15** (1980) 323.

Received 30 September
and accepted 9 November 1981